THE JOURNAL OF PHYSICAL CHEMISTRY B

Article

Cite This: J. Phys. Chem. B 2018, 122, 6148−6155

pubs.acs.org/JPCB

^{19}F Magic Angle Spinning NMR Spectroscopy and Density Functional Theory Calculations of Fluorosubstituted Tryptophans: Integrating Experiment and Theory for Accurate Determination of Chemical Shift Tensors

Manman Lu,[†,‡,∞] Sucharita Sarkar,[†,‡,∞] Mingzhang Wang,[†,‡,∞] Jodi Kraus,[†,∞] Matthew Fritz,[†] Caitlin M. Quinn,[†] Shi Bai,[†] Sean T. Holmes,[†] Cecil Dybowski,[†] Glenn P. A. Yap,[†] Jochem Struppe,[∥] Ivan V. Sergeyev,[∥] Werner Maas,[∥] Angela M. Gronenborn,*[,‡,§] and Tatyana Polenova*[,†,‡]

[†]Department of Chemistry and Biochemistry, University of Delaware, Newark, Delaware 19716, United States

[‡]Pittsburgh Center for HIV Protein Interactions, University of Pittsburgh School of Medicine, 1051 Biomedical Science Tower 3, 3501 Fifth Avenue, Pittsburgh, Pennsylvania 15261, United States

[§]Department of Structural Biology, University of Pittsburgh School of Medicine, 3501 Fifth Avenue, Pittsburgh, Pennsylvania 15261, United States

[∥]Bruker Biospin Corporation, 15 Fortune Drive, Billerica, Massachusetts 01821, United States

Supporting Information

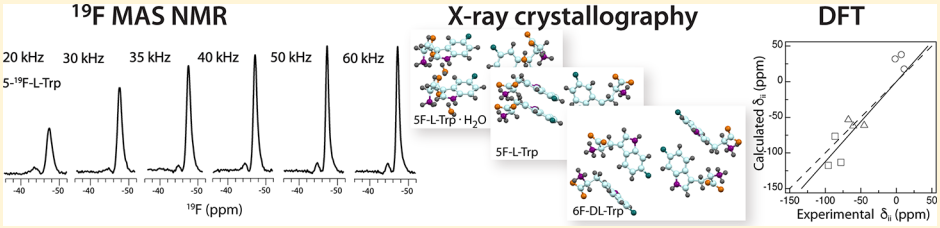

ABSTRACT: The ^{19}F chemical shift is a sensitive NMR probe of structure and electronic environment in organic and biological molecules. In this report, we examine chemical shift parameters of 4F-, 5F-, 6F-, and 7F-substituted crystalline tryptophan by magic angle spinning (MAS) solid-state NMR spectroscopy and density functional theory. Significant narrowing of the ^{19}F lines was observed under fast MAS conditions, at spinning frequencies above 50 kHz. The parameters characterizing the ^{19}F chemical shift tensor are sensitive to the position of the fluorine in the aromatic ring and, to a lesser extent, the chirality of the molecule. Accurate calculations of ^{19}F magnetic shielding tensors require the PBE0 functional with a 50% admixture of a Hartree−Fock exchange term, as well as taking account of the local crystal symmetry. The methodology developed will be beneficial for ^{19}F-based MAS NMR structural analysis of proteins and protein assemblies.

INTRODUCTION

Fluorine, or specifically, the magnetically active ^{19}F isotope, is an excellent NMR probe for applications in biological and biochemical studies because of its favorable magnetic and chemical properties. Being a 100% naturally abundant spin-1/2 nucleus with a very high gyromagnetic ratio (third after ^{3}H and ^{1}H), it possesses 83% sensitivity compared to ^{1}H. Fluorine chemical shifts are exquisitely sensitive to changes in local environment because its magnetic shielding is dominated by a large paramagnetic term: the ^{19}F chemical shift range is over 300 ppm, 30-fold larger than that of ^{1}H.[1,2] Fluorine is absent from virtually all naturally occurring biomolecules, small or large. In addition, fluorine can easily be biosynthetically incorporated into proteins in the context of either natural or unnatural amino acids or attached as a fluorinated tag to reactive amino acids, such as cysteine.[1−5] In particular, tryptophan residues are often chosen for fluorine incorporation because of their relative sparseness in most proteins.[6,7] Biosynthetic incorporation into proteins and peptides using standard *Escherichia coli* expression systems is easy,[3,8−10] and the effects on conformation or biological activity of proteins upon fluorination are small, in most cases.[3]

Indeed, ^{19}F has found interesting applications in NMR spectroscopy of biologically important materials already.[1−5,10−12] In solution, ^{19}F has been used as a probe to investigate protein folding,[4] ligand binding,[10] and conformational dynamics,[2] including exciting applications to membrane proteins, such as G protein-coupled receptors.[13,14] In the solid state, ^{19}F chemical shift probes have been applied to membrane-associated peptides and proteins using oriented

Received: January 12, 2018
Revised: May 11, 2018
Published: May 14, 2018

DOI: 10.1021/acs.jpcb.8b00377
J. Phys. Chem. B 2018, 122, 6148−6155

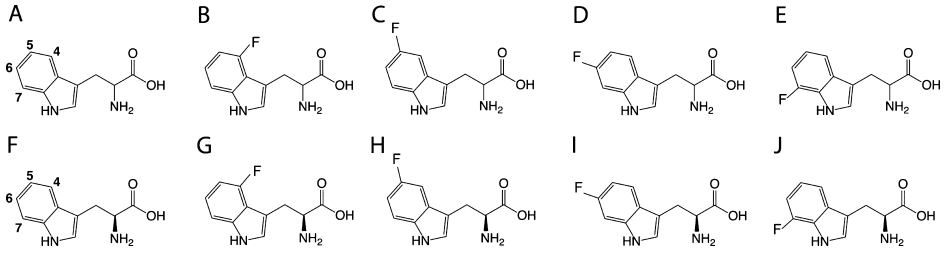

Figure 1. Chemical structures for tryptophan and various fluorotryptophan molecules (A) DL-tryptophan, (B) 4F-DL-tryptophan, (C) 5F-DL-tryptophan, (D) 6F-DL-tryptophan, (E) 7F-DL-tryptophan, (F) L-tryptophan, (G) 4F-L-tryptophan, (H) 5F-L-tryptophan, (I) 6F-L-tryptophan, and (J) 7F-L-tryptophan.

samples and static experiments, as well as magic angle spinning (MAS) NMR spectroscopy.[15−21]

One limitation that prevents the widespread use of fluorine as an NMR reporter in biochemical applications is the lack of a systematic understanding of the relationship between ^{19}F chemical shifts and local environments. This knowledge gap exists because there are, at present, no robust protocols for quantum mechanical calculations of ^{19}F chemical shifts. Such calculations have been traditionally difficult[22,23] because of the stringent requirements on the inclusion of electron-correlation terms, given the large number of electrons and free electron pairs in fluorine. Although earlier studies have suggested that Hartree−Fock (HF) self-consistent-field or post-HF calculations are essential to compute accurate ^{19}F chemical shifts,[22,24] recent reports suggest that density functional theory (DFT) can be used, provided that explicit solvent models are employed[25] and appropriate hybrid functionals with sufficient exact exchange terms are used.[26,27] These developments are very promising.

Another challenge specific to ^{19}F solid-state NMR spectroscopy arises from its generic broad lines,[21] often limiting fluorine-based correlation experiments when multiple sites are present. Currently, the literature on ^{19}F MAS NMR in biological systems is sparse, predominantly reporting on MAS studies at spinning frequencies below 25 kHz, although a recent study demonstrated resolution enhancements for sitagliptin at 35 kHz.[28] Optimal experimental conditions necessary for the acquisition of high-quality datasets still have to be established.

To develop a robust protocol for ^{19}F MAS NMR spectroscopy-based characterization of structure and dynamics in fluorinated solids, it is imperative to examine a sufficiently large number of model systems to benchmark ^{19}F MAS NMR's use for biological applications. In this report, we present a combined ^{19}F MAS NMR and DFT study of fluorosubstituted tryptophans (Figure 1). We assess the dependence of the experimental ^{19}F chemical shift tensor (CST) parameters on the fluorine position in the aromatic ring and the chirality of the tryptophan molecule. For 5F-L-Trp, 5F-L-Trp·H_2O, and 6F-DL-Trp, whose crystal structures we solved, DFT calculations of ^{19}F CST were carried out. Good agreement between experiment and theory was obtained when the PBE0 functional with a 50% admixture of HF exchange terms was employed. On the experimental side, the use of high MAS frequencies of over 50 kHz is essential to obtain sufficiently narrow lines. Overall, the integrated approach presented here should set the stage for a wide variety of applications in organic and biological systems.

MATERIALS AND METHODS

Fluorosubstituted Tryptophans. 4F-DL-tryptophan, 5F-L-tryptophan, and 6F-L-tryptophan were purchased from Sigma-Aldrich. 5F-DL-tryptophan was purchased from MP Biomedicals, LLC (Santa Ana, CA). 6F-DL-tryprophan was purchased from Apollo Scientific Ltd (UK). 7F-DL-tryptophan was purchased from Amatek Chemical Co. Ltd (Hong Kong). For measurements of the powders, all fluorosubstituted tryptophans were used without further purification.

Crystallization of Fluorosubstituted Tryptophans and Crystal Structure Determination. 5F-L-tryptophan, 5F-DL-tryptophan, and 6F-DL-tryptophan were recrystallized from a 30% water/ethanol mixture. Crystals suitable for X-ray diffraction were obtained at ambient temperature. The details of the crystal structure determination are provided in the Supporting Information.

^{19}F MAS NMR Experiments. ^{19}F MAS NMR experiments on 4F-DL-tryptophan, 5F-DL-tryptophan, 5F-L-tryptophan, 6F-DL-tryptophan, 6F-L-tryptophan, and 7F-DL-tryptophan were carried out at room temperature (21 °C) on a 9.4 T NMR spectrometer comprising a wide-bore Magnex Scientific magnet and a Bruker AVANCE console. The spectrometer was equipped with a 3.2 mm Varian T3 MAS HXY probe. The ^{19}F Larmor frequency was 376.476 MHz. The samples comprising 20 mg of either 4F-DL-tryptophan, 5F-DL-tryptophan, 6F-DL-tryptophan, or 6F-L-tryptophan packed in a 3.2 mm Varian rotor. For 5F-L-tryptophan and 7F-DL-tryptophan, 10 and 4 mg of the samples were packed into rotors, respectively. ^{19}F MAS NMR spectra were collected at MAS frequencies of 5, 7, 9, and 11 kHz, controlled to within ±10 Hz by a Tecmag MAS controller. The typical ^{19}F 90° pulse length was 1.4 μs. During the odd-numbered transients, a 180° pulse was applied before the 90° excitation pulse to suppress ^{19}F background signals. The recycle delay was 10 s.

^{19}F MAS NMR experiments on 3.0 mg of 5F-DL-tryptophan, 3.0 mg of 5F-L-tryptophan, 1.8 mg of 6F-DL-tryptophan, and 2.2 mg of 6F-L-tryptophan, respectively, were also carried out on a Varian 14.1 T narrow bore magnet equipped with a Bruker AVIII HD spectrometer operating at 564.278 MHz and outfitted with a 1.3 mm Bruker HCN MAS probe. ^{19}F MAS NMR spectra were collected at MAS frequencies of 8, 11 kHz (except for 5F-DL-tryptophan), 20, 30, 35, 40, 50, and 60 kHz; the frequencies were controlled to within ±5 Hz by a Bruker MAS controller. The typical ^{19}F 90° pulse length was 1.3 μs. The recycle delay was 3 s.

The effects of magnetic field strength and ^{1}H decoupling were assessed using ^{19}F MAS NMR experiments with 5F-DL-tryptophan. MAS NMR experiments were carried out on a 11.7 T wide-bore Bruker AVANCE III spectrometer outfitted with a 2.5 mm MAS HFX probe. Larmor frequencies were 500.1 MHz (^{1}H) and 470.6 MHz (^{19}F). 5F-DL-tryptophan (8 mg) were packed into a 2.5 mm thick-walled Bruker rotor. ^{19}F MAS NMR spectra were collected at MAS frequencies of 5, 7,

DOI: 10.1021/acs.jpcb.8b00377
J. Phys. Chem. B 2018, 122, 6148−6155

Table 1. MAS NMR Experimental and DFT Calculated (ADF) Principal Components of the CST, Isotropic Chemical Shifts, Reduced Anisotropy, and Asymmetry Parameters for the Fluorosubstituted F-DL-Tryptophans and Fluorosubstituted F-L-Tryptophans

		Experiment (MAS NMR)						DFT Calculation (ADF, 4 molecules)					
	Compound	δ_{11} (ppm)	δ_{22} (ppm)	δ_{33} (ppm)	δ_{iso} (ppm)	δ_{σ} (ppm)	η	δ_{11} (ppm)	δ_{22} (ppm)	δ_{33} (ppm)	δ_{iso} (ppm)	δ_{σ} (ppm)	η
Powder	4F-DL-Trp	11.2±1.4	48.3±0.5	-112.8±0.8	-50.0	62.8±0.8	0.9±0.0						
	5F-DL-Trp	4.8±1.3	-60.5±1.0	-86.1±1.2	-47.2	51.8±1.3	0.50±0.03						
	5F-L-Trp	-0.8±3.7	-62.9±1.4	-84.4±4.1	-49.4	48.6±3.7	0.44±0.08						
	6F-DL-Trp	12.9±1.4	-51.2±0.5	-91.6±1.4	-43.3	56.2±1.4	0.72±0.02						
	6F-L-Trp	12.6±1.1	-50.7±2.8	-91.3±1.9	-43.2	55.7±1.2	0.7±0.1						
	7F-DL-Trp	4.6±1.9	-48.3±0.5	-123.3±1.4	-55.7	67.6±1.4	0.8±0.0						
Crystal	5F-L-Trp	-1.7±0.3	-67.5±0.2	-78.0±0.2	-49.1	47.4±0.3	0.2±0.0	31.9	-53.4	-113.2	-44.9	76.8	0.8
	5F-L-Trp·H_2O	6.9±0.5	-60.7±0.3	-86.3±0.4	-46.7	53.6±0.5	0.5±0.0	38.0	-62.1	-76.6	-33.5	71.6	0.2
	6F-DL-Trp*	11.0±0.8	-45.2±0.4	-95.7±0.6	-43.3	54.3±0.8	0.9±0.0	17.8	-61.2	-117.2	-53.6	71.3	0.8
								17.6	-61.4	-117.8	-53.8	71.5	0.8

[a]The DFT calculations of 6F-DL-Trp are reported as the individual values for the D- and L-enantiomers (top and bottom, respectively).

11.111, and 30 kHz, with the frequencies controlled to within ±5 Hz by a Bruker MAS controller. The actual sample temperature was calibrated using KBr as a temperature sensor and was maintained at 20 ± 1 °C throughout the experiments using a Bruker temperature controller. The typical 90° pulse lengths were 2.5 μs (^{1}H) and 2.5 μs (^{19}F). Single-pulse ^{19}F spectra were acquired by using a small-angle excitation pulse with a pulse length of 0.5 μs. ^{1}H TPPM decoupling[29] (91 kHz) was used during the acquisition period. The recycle delay was 3 s.

MAS NMR experiments were also carried out on a 19.96 T Bruker AVANCE III spectrometer operating at 800.095 MHz, outfitted with a 1.9 mm MAS HX probe and a 1.6 mm MAS HFDXY Phoenix probe. 5F-DL-tryptophan (9 mg) were packed into a 1.9 mm thin-wall Bruker rotor. ^{19}F MAS NMR spectra were collected at MAS frequencies of 11, 15, 30, and 40 kHz, and the frequencies were controlled to within ±5 Hz by a Bruker MAS controller. The actual sample temperature was calibrated using KBr as a temperature sensor and was maintained at 25 ± 1 °C throughout the experiments using a Bruker temperature controller. The typical 90° pulse length for ^{19}F was 1.8 μs. During the odd-numbered transients, a 180° pulse was applied before the 90° excitation pulse to suppress ^{19}F background signals. The recycle delay was 3 s.

5F-DL-tryptophan (7.6 mg) were packed into a 1.6 mm Varian rotor. ^{19}F MAS NMR spectra were collected at a MAS frequency of 40 kHz, regulated to within ±5 Hz by a Bruker MAS controller. The typical 90° pulse lengths were 2.7 μs (^{1}H) and 2.7 μs (^{19}F). ^{1}H TPPM decoupling (10 kHz) was used during the acquisition period. The recycle delay was 80 s.

^{19}F chemical shifts were referenced to trifluoroacetic acid (100 μM solution in 25 mM sodium phosphate buffer, pH 6.5), using an external reference (0 ppm).

All ^{19}F MAS spectra were processed using TopSpin. Baseline correction was employed using manually defined baseline points.

Determination of CSTs. The principal components of ^{19}F CSTs were determined by fitting the spinning sideband intensities according to the Herzfeld–Berger protocol.[30] The peak intensities were obtained from TopSpin and were input into the HBA program, version 1.7.5.[31]

DFT Calculations. ^{19}F magnetic shielding tensor calculations were carried out on 5F-L-Trp·H_2O, 5F-DL-Trp (L-form), and 6F-DL-Trp. For each, molecular clusters comprising four molecules were generated from the crystal structures with GaussView, the graphical interface in Gaussian 09[32] (Figure 4A–C).

All-atom geometry optimizations were carried out in Gaussian 09 using the B3LYP functional and 6-31G basis set. The ^{19}F magnetic shielding tensor calculations were performed with the Amsterdam DFT suite of programs[33] (ADF2017), using a hybrid PBE0 functional with 50% HF exchange, and a TZ2P all-electron basis set (no frozen core). The numerical quality was set to "very good" for each calculation using Becke integration. Magnetic shielding tensors were calculated only for the central fluorine atoms.

The ^{19}F chemical shifts were referenced by converting absolute magnetic shieldings σ into chemical shifts, using the relation $\delta_i = \sigma_{ref} - \sigma_i$, with the value of σ_{ref} determined by linear regression between calculated and experimental shifts.[34]

SIMPSON and SIMMOL Calculations. Calculations were performed for recrystallized 5F-L-Trp·H_2O, 5F-DL-Trp (L-form), and 6F-DL-tryptophan. One fluorine in the crystal structure was chosen as the central atom, and all other neighboring fluorines within 6 Å radius were considered for calculating dipolar coupling tensors. The SIMMOL program[35] reads the atomic coordinates of the selected fluorines in the PDB format, from which it generates dipolar couplings and Euler angles.

The spectra of the crystals were simulated in SIMPSON.[36] The experimental chemical shift anisotropy (CSA) tensors (Table 1) at 14.1 T (^{19}F Larmor frequency of 564.278 MHz) and a MAS frequency of 11 kHz were used, with and without the F–F couplings added from the X-ray structures.

The peak intensities of the simulated spectra were obtained using NMRDRAW.[37] These intensities and the isotropic chemical shifts (Table 1) were used in Herzfeld–Berger analysis for extracting the principal components of the tensors, the reduced anisotropy, and the asymmetry parameter.

DOI: 10.1021/acs.jpcb.8b00377
J. Phys. Chem. B 2018, 122, 6148–6155

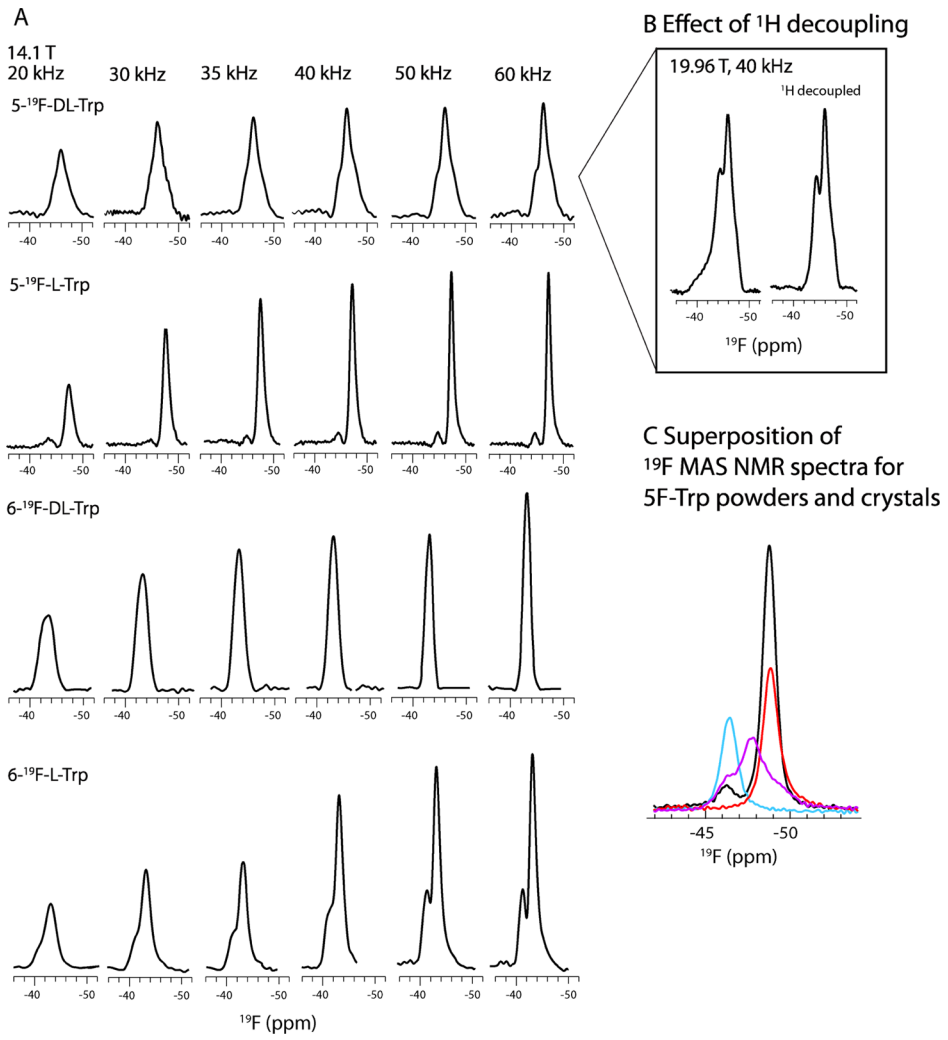

Figure 2. (A) MAS frequency dependence of the linewidth and signal intensity of fluorosubstituted tryptophan crystalline powders (bottom to top): 6F-L-tryptophan, 6F-DL-tryptophan, 5F-L-tryptophan, and 5F-DL-tryptophan. 1D ^{19}F spectra were acquired at 14.1 T (564.278 MHz ^{19}F Larmor frequency) and MAS frequencies of 20, 30, 35, 40, 50, and 60 kHz. (B) For 5F-DL-tryptophan, ^{19}F 1D spectra were also acquired at 19.96 T (800.095 MHz ^{19}F Larmor frequency) and a MAS frequency of 40 kHz, with (right spectrum) and without ^{1}H decoupling (left spectrum). (C) Superposition of the ^{19}F MAS NMR spectra for different forms of 5F-Trp (powder vs crystal): 5F-L-tryptophan powder (black), 5F-L-tryptophan monohydrate crystals (blue), 5F-L-tryptophan crystals (red), and 5F-DL-tryptophan powder (magenta). The chemical shift of −46.4 ppm likely corresponds to the monohydrate form.

RESULTS

^{19}F MAS NMR Spectra of Fluorosubstituted Tryptophans. ^{19}F MAS NMR spectra of powder and crystalline tryptophan with fluorine substitutions in the 4-, 5-, 6-, and 7-positions of the indole ring were acquired at magnetic field strengths of 9.4, 14.1, and 19.96 T and at MAS frequencies ranging from 5 to 60 kHz (Figures 2, S1 and S2 of the Supporting Information). Increasing the MAS frequency from 20 to 60 kHz, in the absence of proton decoupling, results in dramatic line narrowing and increases in peak intensity because of improved efficiency of the rotational averaging of ^{19}F CSA and ^{1}H−^{19}F/^{19}F−^{19}F dipolar interactions (Figure 2; Table S1 of the Supporting Information). As can easily be appreciated from the comparison provided in Figure 2B, the spectral resolution attained for 5F-DL-tryptophan at 14.1 T and a MAS frequency of 60 kHz in the absence of decoupling is similar to that observed in experiments at 19.96 T and a MAS frequency of 40 kHz, in the presence of ^{1}H decoupling. At 60 kHz, the linewidths are ∼1 ppm for all samples under investigation, indicating that the non-recrystallized tryptophan powders are crystalline. This was confirmed by X-ray powder diffraction of 4F-DL-, 5F-DL-, 6F-L-, and 6F-DL-tryptophans (Figure S3 of the Supporting Information).

The above findings are important: they demonstrate that ^{19}F MAS NMR spectroscopy can be widely applied, even in the absence of specialized probes that are capable of ^{1}H decoupling while detecting ^{19}F.

Experimental CSTs of Fluorosubstituted Tryptophans. To determine accurate ^{19}F chemical shift parameters of the different fluorosubstituted tryptophans, we acquired ^{19}F MAS spectra at different magnetic field strengths (9.4, 14.1, and 19.96 T) and at MAS frequencies ranging between 5 and 60 kHz. ^{19}F isotropic shifts are summarized in Table 1. The MAS isotropic shifts of 4F-Trp and 6F-Trp are similar to the solution NMR values, to within 1 ppm, for fluorosubstituted L-Trp molecules.[5] For 7F-L-Trp, a difference of 3.1 ppm is observed (the solution NMR shift is −58.8 ppm). Isotropic shifts range from −41.4 to −59.6 ppm, influenced by the position of the fluorine in the indole ring and local environments. Interestingly,

DOI: 10.1021/acs.jpcb.8b00377
J. Phys. Chem. B 2018, 122, 6148−6155

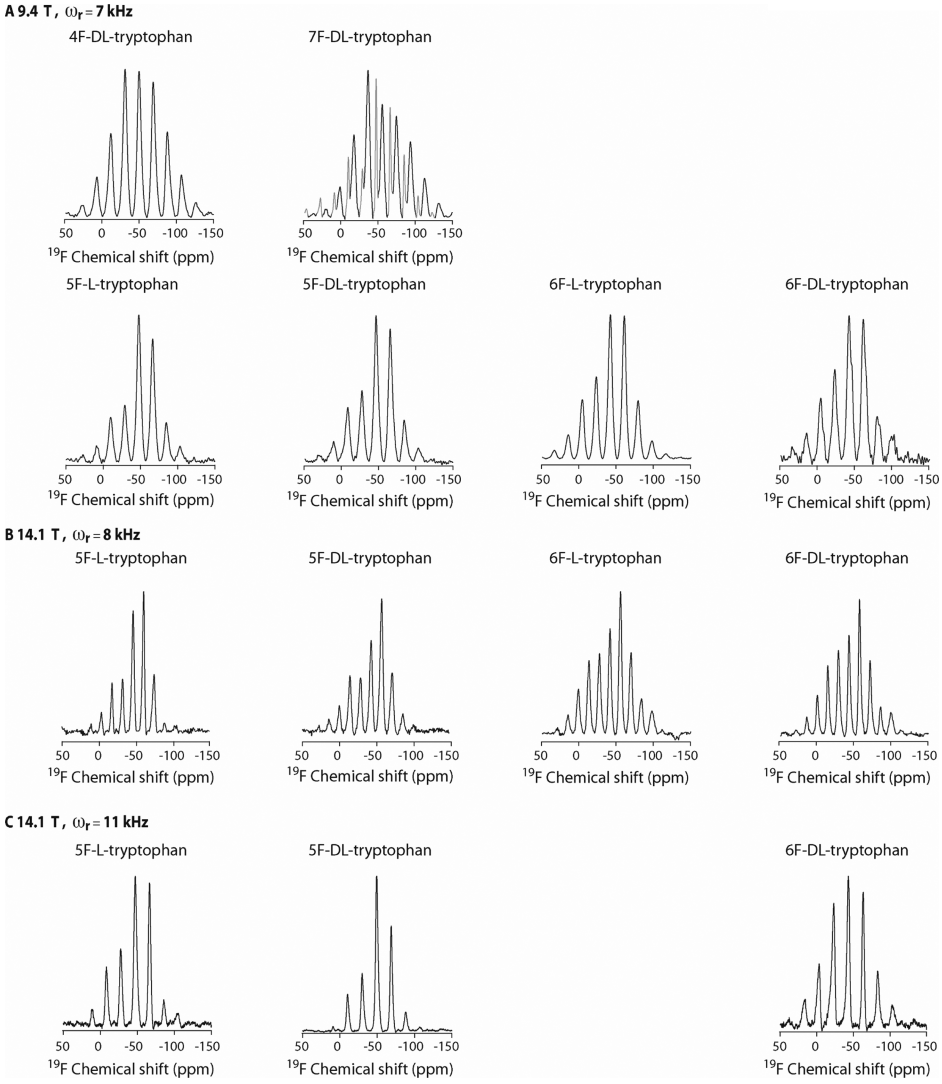

Figure 3. ^{19}F MAS NMR spectra of microcrystalline powders of fluorosubstituted tryptophans acquired at (A) 9.4 T and 7 kHz, (B) 14.1 T and 8 kHz, and (C) 14.1 T and 11 kHz. The peaks colored in light gray in (A) arise from the ^{19}F signal of the sample spacer.

MAS isotropic shifts appear to be sensitive to the hydration state of the molecule, as seen for 5F-Trp (Figure 2C). The shift of −46.4 ppm appears to be associated with the monohydrate form of the 5F-L-Trp. The chemical shift of −48.7 ppm was observed in microcrystalline nonhydrated powders of 5F-DL-Trp (minor peak) and 5F-L-Trp (major peak) and is the only species in the recrystallized 5F-DL-Trp. Interestingly, a pure L-enantiomer was detected in the single-crystal X-ray diffraction experiments. The L-conformation was assigned based on the handedness that gave values of the Flack parameter closest to zero, albeit the standard error values were high (see the Supporting Information). The major resonance in the 5F-DL-Trp powder (−47.7 ppm) is assigned to the D-enantiomer by exclusion.

Representative spectra acquired at MAS frequencies ranging between 5 and 15 kHz are provided in Figure 3 (all spectra are shown in Figures S1 and S2 of the Supporting Information). ^{19}F CSTs have been previously determined for 5F-L, 5F-DL-, 6F-L-, and 6F-DL-tryptophan, and the reported values for the reduced anisotropy parameter, δ_σ, for 5F-DL-Trp differ by 2.2 ppm for the MAS[38] versus the single-crystal static[39] NMR study. These differences may be because of experimental uncertainties or, more likely, different crystal forms. In the present work, we recorded multiple MAS spectra for each compound, which permitted us to extract accurate CST parameters and assess the range of experimental errors in these measurements.

Experimental CST parameters were obtained by analyzing the spinning sideband intensities using the Herzfeld−Berger protocol.[30] All values are summarized in Table 1. The reduced anisotropy parameters range between 48.6 and 67.6 ppm. The positioning of the fluorine in the indole ring exerts the largest effect on the shift, and smaller, but distinct, differences (0.5−3.2 ppm) are observed for molecules of different chirality. All of the tensors are rhombic, with the asymmetry parameters ranging from 0.44−0.50 (for 5F-Trp) to 0.95 (for 4F-Trp). Overall, pronounced differences in the CST parameters are observed, underscoring the remarkably high sensitivity of fluorine CSTs to local electronic structure.

CST parameters for every fluorosubstituted tryptophan and each set of spectra (Table S2 of the Supporting Information) permitted us to evaluate the experimental errors carefully. The experimental uncertainties in the ^{19}F reduced anisotropy parameter δ_σ, extracted from the spinning sideband analyses

DOI: 10.1021/acs.jpcb.8b00377
J. Phys. Chem. B 2018, 122, 6148−6155

Table 2. Contribution of Homonuclear F−F Dipolar Couplings to the Experimental ^{19}F MAS NMR Lineshapes of Crystalline 5F-L-Trp, 5F-L-Trp·H_2O, and 6F-DL-Trp[a]

compound	closest F−F distance (Å)	F−F dipolar coupling (Hz)	δ_{11} (ppm)	δ_{22} (ppm)	δ_{33} (ppm)	δ_{σ} (ppm)	η
5F-L-Trp	4.5	−1179.0	−1.6 ± 0.2	−67.2 ± 0.1	−78.5 ± 0.1	47.5 ± 0.2	0.2 ± 0.0
			−1.7 ± 0.2	−67.4 ± 0.1	−78.2 ± 0.1	47.4 ± 0.2	0.2 ± 0.0
5F-L-Trp·H_2O	4.6	−1082.4	6.9 ± 0.1	−60.0 ± 0.1	−87.1 ± 0.1	53.6 ± 0.1	0.5 ± 0.0
			6.9 ± 0.1	−60.0 ± 0.1	−87.0 ± 0.1	53.6 ± 0.1	0.5 ± 0.0
6F-DL-Trp	2.9	−4134.8	11.8 ± 0.3	−45.1 ± 0.2	−96.6 ± 0.2	55.1 ± 0.3	0.9 ± 0.0
			10.8 ± 0.1	−45.2 ± 0.1	−95.6 ± 0.1	54.2 ± 0.1	0.9 ± 0.0

[a]Experimental CST components and F−F homonuclear dipolar coupling contributions were extracted using SIMPSON. ^{19}F MAS NMR simulations for the ^{19}F crystals were carried out at 14.1 T (^{19}F Larmor frequency of 564.278 MHz) and a MAS frequency of 11 kHz. ^{19}F MAS NMR simulations for the clusters generated from ^{19}F-substituted on non-F tryptophan crystals were carried out at 9.4 T (376.476 MHz ^{19}F Larmor frequency) and a MAS frequency of 7 kHz.

of the MAS spectra, are on the order of 0.8−3.7 ppm or 5−7% of the total magnitude of δ_{σ}. This error range is reasonable because accurate values rely on the intensities of the outer, low-intensity sidebands, whose quantification becomes more difficult for slower MAS frequencies. We also considered the effect of ^{19}F−^{19}F homonuclear couplings on the spinning sideband intensities for the 5F-DL-Trp, 5F-L-Trp·H_2O, and 6F-DL-Trp crystalline samples, whose structures we solved (Table 2). For 5F-DL-Trp and 5F-L-Trp·H_2O, the effects are negligible. For 6F-DL-Trp, the effects were small, but discernible, in the absence of ^{1}H decoupling and need to be considered when CST parameters are extracted from the spectra. Overall, the CSTs for 5F-L/DL and 6F-L/DL tryptophan determined here are in good agreement with the published values,[38,40] within experimental uncertainty.

DFT Calculations of ^{19}F CSTs of Fluorosubstituted Tryptophans. Recent studies indicate that in the DFT calculations of ^{19}F chemical shifts in solids, using the Amsterdam Density Functional (ADF) program with the PBE0 functional,[41] a 50% HF exchange admixture term and an all-electron Slater-type (TZ2P) basis set yields values in reasonable agreement with experiment, if the molecular clusters reflect the overall symmetry of the crystal lattice.[26,27] As revealed by the XRD patterns (Figure S3 of the Supporting Information), the crystal forms of the powdered fluorosubstituted tryptophans are not the same as the reported X-ray structures of the parent L-tryptophan,[42] DL-tryptophan,[43] or 5F-DL-tryptophan[39] in the Cambridge crystallographic data base. We therefore restricted our chemical shift calculations to 5F-L-Trp, 5F-L-Trp·H_2O, and 6F-DL-Trp crystals, whose structures we solved.

Four molecule clusters were constructed, using the crystal coordinates. The molecular geometries of these clusters are shown in Figure 4A−C, and the results of the chemical shift calculations are summarized in Figure 4D and Table 1. Gratifyingly, the calculated tensors are in reasonable overall agreement with the experimental values with a slope of 1.12 for the correlation between experimental and calculated CST components. Given that we restricted our calculations to the 5F- and 6F-substituted tryptophans for which crystal structures were solved, the chemical shift range is too small (5.8 and 6.9 ppm for the isotropic shift and reduced anisotropy, respectively) to conduct rigorous analyses with respect to the quality of the calculations. Nevertheless, the slope of 1.12 for the principal components of the CST in the four-molecule clusters suggests that these models do not fully capture the long-range electrostatic effects on the magnetic shielding. This is in line with previous studies[26,27] and a result of the fact that

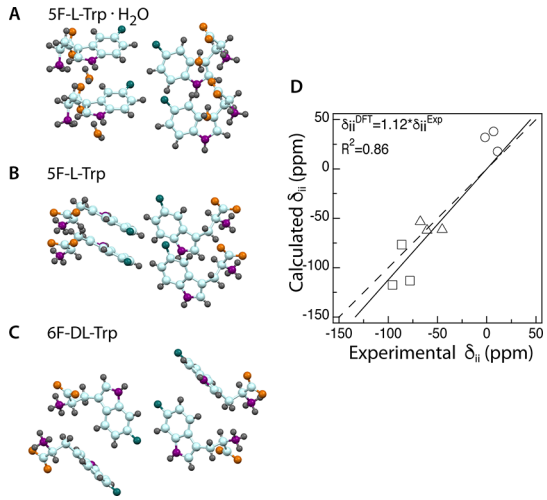

Figure 4. (A−C) Molecular clusters of (A) 5F-L-tryptophan monohydrate, (B) 5F-L-tryptophan, and (C) 6F-DL-tryptophan generated from the crystal structure coordinates. Fluorine atoms are shown in deep teal, nitrogen atoms in purple, oxygen atoms in orange, carbons in pale cyan, and hydrogen atoms in dark gray. (D) Correlation between experimental and calculated ^{19}F CSTs for the three model clusters in fluorosubstituted tryptophans. The principal components of magnetic shielding tensors δ_{11}, δ_{22}, and δ_{33} are shown as circles, triangles, and squares, respectively. The best fit is shown as a solid line and the ideal $y = x$ as a dashed line. All calculations were performed with the ADF suite of programs.

fluorine magnetic shieldings are dominated by long-range electrostatic contributions. Future studies will be conducted on larger molecular cluster models (15−17 molecules; 400−500 atoms) and on 4F- and 7F-substituted crystalline tryptophans of known structures.

It should also be noted that periodic structure calculations do not yield a better agreement with the experiment, and large cluster calculations using appropriately constructed symmetry-adapted molecular clusters and high level of theory appear to be necessary, as we have demonstrated previously for fluorine in a wide variety of environments.[27]

DISCUSSION

Solid-state ^{19}F NMR chemical shift parameters were determined for a series of crystalline tryptophans containing fluorine at the 4-, 5-, 6-, and 7-positions. The isotropic and anisotropic components of the CSTs in these molecules are very sensitive to the positioning of the fluorine atom in the indole ring, thereby making fluorotryptophans excellent ^{19}F

DOI: 10.1021/acs.jpcb.8b00377
J. Phys. Chem. B 2018, 122, 6148−6155

NMR probes in protein studies, as has been previously shown for solution NMR studies.[5,10] One important result of the current work is the demonstration that the ^{19}F lines are narrow at a MAS frequency of 60 kHz, diminishing the need for ^{1}H decoupling. This observation holds true for proteins as well, making ^{19}F MAS NMR investigations on a broad range of large biological molecules and assemblies practical and accessible to many laboratories. Although we currently do not have access to ^{19}F "ultrafast" MAS probes (frequencies of 100−110 kHz), it is possible to extrapolate our findings to MAS frequencies above 100 kHz, where, similar to the ^{1}H ultrafast MAS NMR studies of organic molecules and proteins,[44,45] further line narrowing and sensitivity gains are expected.

In addition to our experimental studies by MAS NMR spectroscopy, we also performed DFT calculations of CSTs in fluorosubstituted tryptophan crystals with known structures. This investigation was prompted by the paucity of literature on quantum chemical calculations of ^{19}F NMR parameters, both for organic and biological systems. Our findings demonstrate that DFT can be used successfully for the calculation of ^{19}F CSA parameters, provided a high percentage (50%) of the HF exchange term is used in the functional, and the wave function is expanded on a basis of Slater-type atomic orbitals. Future investigations for improving the accuracy of these calculations will focus on large molecular clusters that reflect the overall crystal symmetry and capture long-range electrostatic effects.

CONCLUSIONS

Our integrated experimental ^{19}F MAS NMR and computational DFT study of fluorosubstituted tryptophans permitted a thorough evaluation of the influence of the local environment on the ^{19}F CST and demonstrated the advantages of fast-MAS (60 kHz or greater) experiments for studying ^{19}F-containing solid biological materials. The approach presented here is broadly applicable for the characterization of other organic solids by ^{19}F MAS NMR spectroscopy and holds particular promise for studies employing fluorosubstituted tryptophans in proteins and protein assemblies.

ASSOCIATED CONTENT

Supporting Information

The Supporting Information is available free of charge on the ACS Publications website at DOI: 10.1021/acs.jpcb.8b00377.

MAS NMR spectra of fluorosubstituted tryptophans at several magnetic fields and MAS frequencies; powder XRD patterns; MAS frequency and magnetic field dependence of the sensitivity of the ^{19}F MAS NMR experiments; summary of experimental CSA parameters at various field strengths; and for recrystallized 5F-DL-Trp, 5F-L-Trp·H_2O, and 6F-DL-Trp—(i) X-ray structure determination protocols; (ii) crystal data and structure refinement parameters; (iii) atomic coordinates and equivalent isotropic displacement parameters; (iv) bond lengths and bond angles; (v) anisotropic displacement parameters; and (vi) hydrogen coordinates and isotropic displacement parameters (PDF)

AUTHOR INFORMATION

Corresponding Authors

*E-mail: amg100@pitt.edu. Phone: (412) 648-9959 (A.M.G.).
*E-mail: tpolenov@udel.edu. Phone: (302) 831-1968 (T.P.).

ORCID

Cecil Dybowski: 0000-0002-0557-8915
Angela M. Gronenborn: 0000-0001-9072-3525
Tatyana Polenova: 0000-0002-0346-1131

Author Contributions

∞M.L., S.S., M.W., and J.K. contributed equally. A.M.G. and T.P. conceived and directed the project. M.L., S.S., M.W., J. K., M.F., C.M.Q., and S.B. performed NMR experiments. J.K. crystallized the fluorinated tryptophans, G.Y. solved the crystal structures, and S.S. performed DFT calculations. C.D. supervised the calculations. S.T.H. and J.S. contributed to the interpretation of the results. T.P., A.M.G., and C.D. took the lead in writing the manuscript. All authors discussed the results and commented on the manuscript.

Notes

The authors declare no competing financial interest.

ACKNOWLEDGMENTS

We thank Professor Eric Bloch for the use of the powder XRD instrumentation. This work was supported by the National Science Foundation (NSF grant CHE-1708773 to A.M.G. and T.P.) and by the National Institutes of Health (NIGMS and NIAID, grant P50 GM082251, Technology Development Project on MAS NMR). J.K. was supported by National Science Foundation Graduate Research Fellowship (#1247394). We acknowledge the National Science Foundation (NSF grant CHE-0959496) for the acquisition of the 850 MHz NMR spectrometer at the University of Delaware and the National Institutes of Health (NIH grants P30GM103519 and P30GM110758) for the support of core instrumentation infrastructure at the University of Delaware.

REFERENCES

(1) Gakh, Y. G.; Gakh, A. A.; Gronenborn, A. M. Fluorine as an NMR Probe for Structural Studies of Chemical and Biological Systems. *Magn. Reson. Chem.* **2000**, *38*, 551−558.

(2) Sharaf, N. G.; Ishima, R.; Gronenborn, A. M. Conformational Plasticity of the NNRTI-Binding Pocket in HIV-1 Reverse Transcriptase: A Fluorine Nuclear Magnetic Resonance Study. *Biochemistry* **2016**, *55*, 3864−3873.

(3) Campos-Olivas, R.; Aziz, R.; Helms, G. L.; Evans, J. N. S.; Gronenborn, A. M. Placement of ^{19}F into the Center of GB1: Effects on Structure and Stability. *FEBS Lett.* **2002**, *517*, 55−60.

(4) Matei, E.; André, S.; Glinschert, A.; Infantino, A. S.; Oscarson, S.; Gabius, H.-J.; Gronenborn, A. M. Fluorinated Carbohydrates as Lectin Ligands: Dissecting Glycan-Cyanovirin Interactions by Using F-19 NMR Spectroscopy. *Chem.—Eur. J.* **2013**, *19*, 5364−5374.

(5) Matei, E.; Gronenborn, A. M. F-19 Paramagnetic Relaxation Enhancement: A Valuable Tool for Distance Measurements in Proteins. *Angew. Chem., Int. Ed.* **2016**, *55*, 150−154.

(6) Carugo, O. Amino Acid Composition and Protein Dimension. *Protein Sci.* **2008**, *17*, 2187−2191.

(7) Gaur, R. K. Amino Acid Frequency Distribution among Eurkaryotic Proteins. *IIOAB J.* **2014**, *5*, 6−11.

(8) Clore, G. M.; Gronenborn, A. M.; Birdsall, B.; Feeney, J.; Roberts, G. C. K. ^{19}F-NMR Studies of 3',5'-Difluoromethotrexate Binding to Lactobacillus casei Dihydrofolate Reductase - Molecular Motion and Coenzyme-Induced Conformational Changes. *Biochem. J.* **1984**, *217*, 659−666.

(9) Crowley, P. B.; Kyne, C.; Monteith, W. B. Simple and Inexpensive Incorporation of ^{19}F-Tryptophan for Protein NMR Spectroscopy. *Chem. Commun.* **2012**, *48*, 10681−10683.

(10) Sharaf, N. G.; Gronenborn, A. M. ^{19}F-Modified Proteins and ^{19}F-Containing Ligands as Tools in Solution NMR Studies of Protein Interactions. In *Isotope Labeling of Biomolecules—Labeling Methods*;

DOI: 10.1021/acs.jpcb.8b00377
J. Phys. Chem. B 2018, 122, 6148−6155

Kelman, Z., Ed.; Elsevier Academic Press Inc: San Diego, 2015; Vol. *565*, pp 67−95.
(11) Kitevski-LeBlanc, J. L.; Prosser, R. S. Current Applications of ^{19}F NMR to Studies of Protein Structure and Dynamics. *Prog. Nucl. Magn. Reson. Spectrosc.* **2012**, *62*, 1−33.
(12) Judge, P. J.; Watts, A. Recent contributions from solid-state NMR to the understanding of membrane protein structure and function. *Curr. Opin. Chem. Biol.* **2011**, *15*, 690−695.
(13) Didenko, T.; Liu, J. J.; Horst, R.; Stevens, R. C.; Wüthrich, K. Fluorine-19 NMR of Integral Membrane Proteins Illustrated with Studies of GPCRs. *Curr. Opin. Struct. Biol.* **2013**, *23*, 740−747.
(14) Prosser, R. S.; Luchette, P. A.; Westerman, P. W. Using O-2 to Probe Membrane Immersion Depth by ^{19}F NMR. *Proc. Natl. Acad. Sci. U.S.A.* **2000**, *97*, 9967−9971.
(15) Koch, K.; Afonin, S.; Ieronimo, M.; Berditsch, M.; Ulrich, A. S. Solid-State ^{19}F NMR of Peptides in Native Membranes. In *Solid State Nmr*; Chan, J. C. C., Ed.; Springer-Verlag Berlin: Berlin, 2012; Vol. *306*, pp 89−118.
(16) Wadhwani, P.; Strandberg, E.; Heidenreich, N.; Bürck, J.; Fanghänel, S.; Ulrich, A. S. Self-Assembly of Flexible Beta-Strands into Immobile Amyloid-Like beta-Sheets in Membranes As Revealed by Solid-State ^{19}F NMR. *J. Am. Chem. Soc.* **2012**, *134*, 6512−6515.
(17) Buffy, J. J.; Waring, A. J.; Hong, M. Determination of Peptide Oligomerization in Lipid Bilayers Using ^{19}F Spin Diffusion NMR. *J. Am. Chem. Soc.* **2005**, *127*, 4477−4483.
(18) Luo, W.; Mani, R.; Hong, M. Side-chain Conformation of the M2 Transmembrane Peptide Proton Channel of Influenza A Virus from ^{19}F Solid-State NMR. *J. Phys. Chem. B* **2007**, *111*, 10825−10832.
(19) Su, Y.; DeGrado, W. F.; Hong, M. Orientation, Dynamics, and Lipid Interaction of an Antimicrobial Arylamide Investigated by ^{19}F and ^{31}P Solid-State NMR Spectroscopy. *J. Am. Chem. Soc.* **2010**, *132*, 9197−9205.
(20) Hong, M.; Schmidt-Rohr, K. Magic-Angle-Spinning NMR Techniques for Measuring Long-Range Distances in Biological Macromolecules. *Acc. Chem. Res.* **2013**, *46*, 2154−2163.
(21) Hellmich, U. A.; Pfleger, N.; Glaubitz, C. ^{19}F MAS NMR on Proteorhodopsin: Enhanced Protocol for Site-Specific Labeling for General Application to Membrane Proteins. *Photochem. Photobiol.* **2009**, *85*, 535−539.
(22) Harding, M. E.; Lenhart, M.; Auer, A. A.; Gauss, J. Quantitative Prediction of Gas-Phase ^{19}F Nuclear Magnetic Shielding Constants. *J. Chem. Phys.* **2008**, *128*, 244111.
(23) Sanders, L. K.; Oldfield, E. Theoretical Investigation of ^{19}F NMR Chemical Shielding Tensors in Fluorobenzenes. *J. Phys. Chem. A* **2001**, *105*, 8098−8104.
(24) Elavarasi, S. B.; Dorai, K. Characterization of the ^{19}F Chemical Shielding Tensor Using Cross-Correlated Spin Relaxation Measurements and Quantum Chemical Calculations. *Chem. Phys. Lett.* **2010**, *489*, 248−253.
(25) Isley, W. C.; Urick, A. K.; Pomerantz, W. C. K.; Cramer, C. J. Prediction of ^{19}F NMR Chemical Shifts in Labeled Proteins: Computational Protocol and Case Study. *Mol. Pharm.* **2016**, *13*, 2376−2386.
(26) Holmes, S. T.; Iuliucci, R. J.; Mueller, K. T.; Dybowski, C. Critical Analysis of Cluster Models and Exchange-Correlation Functionals for Calculating Magnetic Shielding in Molecular Solids. *J. Chem. Theory Comput.* **2015**, *11*, 5229−5241.
(27) Alkan, F.; Holmes, S. T.; Dybowski, C. Role of Exact Exchange and Relativistic Approximations in Calculating ^{19}F Magnetic Shielding in Solids Using a Cluster Ansatz. *J. Chem. Theory Comput.* **2017**, *13*, 4741−4752.
(28) Roos, M.; Wang, T.; Shcherbakov, A. A.; Hong, M. Fast Magic-Angle-Spinning ^{19}F Spin Exchange NMR for Determining Nanometer ^{19}F-^{19}F Distances in Proteins and Pharmaceutical Compounds. *J. Phys. Chem. B* **2018**, *122*, 2900−2911.
(29) Bennett, A. E.; Rienstra, C. M.; Auger, M.; Lakshmi, K. V.; Griffin, R. G. Heteronuclear Decoupling in Rotating Solids. *J. Chem. Phys.* **1995**, *103*, 6951−6958.
(30) Herzfeld, J.; Berger, A. E. Sideband intensities in NMR spectra of samples spinning at the magic angle. *J. Chem. Phys.* **1980**, *73*, 6021−6030.
(31) Eichele, K. *HBA, 1.7.5*; Universität Tübingen, 2015.
(32) Frisch, M. J.; Trucks, G. W.; Schlegel, H. B.; Scuseria, G. E.; Robb, M. A.; Cheeseman, J. R.; Scalmani, G.; Barone, V.; Mennucci, B.; Petersson, G. A.; et al. *Gaussian 09*, Revision B.01: Wallingford CT, 2009.
(33) te Velde, G.; Bickelhaupt, F. M.; Baerends, E. J.; Guerra, C. F.; van Gisbergen, S. J. A.; Snijders, J. G.; Ziegler, T. Chemistry with ADF. *J. Comput. Chem.* **2001**, *22*, 931−967.
(34) Baias, M.; Dumez, J.-N.; Svensson, P. H.; Schantz, S.; Day, G. M.; Emsley, L. De Novo Determination of the Crystal Structure of a Large Drug Molecule by Crystal Structure Prediction-Based Powder NMR Crystallography. *J. Am. Chem. Soc.* **2013**, *135*, 17501−17507.
(35) Bak, M.; Schultz, R.; Vosegaard, T.; Nielsen, N. C. Specification and Visualization of Anisotropic Interaction Tensors in Polypeptides and Numerical Simulations in Biological Solid-State NMR. *J. Magn. Reson.* **2002**, *154*, 28−45.
(36) Bak, M.; Rasmussen, J. T.; Nielsen, N. C. SIMPSON: A General Simulation Program for Solid-State NMR Spectroscopy. *J. Magn. Reson.* **2011**, *213*, 366−400.
(37) Delaglio, F.; Grzesiek, S.; Vuister, G.; Zhu, G.; Pfeifer, J.; Bax, A. NMRPipe: A Multidimensional Spectral Processing System Based on UNIX Pipes. *J. Biomol. NMR* **1995**, *6*, 277−293.
(38) Dürr, U. H. N.; Grage, S. L.; Witter, R.; Ulrich, A. S. Solid-State ^{19}F NMR Parameters of Fluorine-Labeled Amino Acids. Part I: Aromatic Substituents. *J. Magn. Reson.* **2008**, *191*, 7−15.
(39) Zhao, X.; DeVries, J. S.; McDonald, R.; Sykes, B. D. Determination of the ^{19}F NMR Chemical Shielding Tensor and Crystal Structure of 5-Fluoro-DL-Tryptophan. *J. Magn. Reson.* **2007**, *187*, 88−96.
(40) Zhao, G.; Perilla, J. R.; Yufenyuy, E. L.; Meng, X.; Chen, B.; Ning, J.; Ahn, J.; Gronenborn, A. M.; Schulten, K.; Aiken, C.; et al. Mature HIV-1 Capsid Structure by Cryo-Electron Microscopy and All-Atom Molecular Dynamics. *Nature* **2013**, *497*, 643−646.
(41) Adamo, C.; Barone, V. Toward Reliable Density Functional Methods Without Adjustable Parameters: The PBE0 Model. *J. Chem. Phys.* **1999**, *110*, 6158−6170.
(42) Görbitz, C. H.; Törnroos, K. W.; Day, G. M. Single-Crystal Investigation of L-Tryptophan with Z' = 16. *Acta Crystallogr., Sect. B: Struct. Sci.* **2012**, *68*, 549−557.
(43) Hübschle, C. B.; Messerschmidt, M.; Luger, P. Crystal Structure of DL-Tryptophan at 173 K. *Cryst. Res. Technol.* **2004**, *39*, 274−278.
(44) Andreas, L. B.; Le Marchand, T.; Jaudzems, K.; Pintacuda, G. High-Resolution Proton-Detected NMR of Proteins at Very Fast MAS. *J. Magn. Reson.* **2015**, *253*, 36−49.
(45) Struppe, J.; Quinn, C. M.; Lu, M.; Wang, M.; Hou, G.; Lu, X.; Kraus, J.; Andreas, L. B.; Stanek, J.; Lalli, D.; et al. Expanding the Horizons for Structural Analysis of Fully Protonated Protein Assemblies by NMR Spectroscopy at MAS Frequencies Above 100 kHz. *Solid State Nucl. Magn. Reson.* **2017**, *87*, 117−125.

DOI: 10.1021/acs.jpcb.8b00377
J. Phys. Chem. B 2018, 122, 6148−6155